Heat transfer characteristics of dry ice-gas flow in the evaporator of a CO2 ultra-low temperature cascade refrigeration system

Xiao-Dong Niu[a*], Hiroshi Yamaguchi[a], Petter Nekså[b], Kenichi Sekimoto[a]

[a]Energy Conversion research Center, Doshisha University, Kyoto, Japan

[b]SINTEF Energy Research, NO-7465 Trondheim, Norway

Abstract

The heat transfer behaviors of CO_2 dry ice-gas two-phase flow have significant effects on the performance of some new refrigeration systems. In this paper, a series experiment of the local heat transfer characteristics of the CO_2 dry ice-gas flow in the trans-triple-point cycle of a CO_2 ultra-low temperature cascade refrigeration system is performed by varying condensation temperatures, rotational frequency of the compressor and opening of the expansion valve. From the obtained results, the local heat transfer coefficient and wall temperature along the evaporator show greatly complicated behaviors due to the fact that the dry ice particles are condensed, sublimated and interactive with CO_2 gas flow in the evaporator tube.

Keywords: Heat transfer; Ultra-low temperature cascade refrigeration system; Dry ice-gas flow.

* Author to whom correspondence should be addressed. Email address: xniu@mail.doshisha.ac.jp

1. Introduction

Continuously environmental concerns on the ozone layer depletion and global warming have spurred extensive researches on looking for "environmentally friendly" refrigerant alternatives around the world in recent years (ASHRAE handbook), and a ecologically safe and natural refrigerant, CO_2, has received significant attentions in developing various energy conversion systems (Lorentzen 1990, 1993, 1994; Nekså et al. 1998, 2002; Hafner 1998; Liao et al. 2002; Saikawa 2004; Girolto et al. 2004; Cechinato et al. 2005; Rieberer 2005; Stene 2005; Zhang et al. 2005; Kim et al. 2004, 2009). Compared to other typical natural fluids, CO_2 seems to be more favorable as a refrigerant fluid due to it having well thermodynamic and transport properties in terms of heat transfer and pressure drop (Kim et al. 2004; Zhang & Yamaguchi 2007). Due to these merits, using CO_2 in compression refrigeration and heat pump systems seem to be the most promising applications of energy conversion (Hafner 1998; Cechinato et al. 2005; Stene 2005). However, Most of the refrigeration processes and equipments using CO_2 as a working fluid can only achieve the refrigeration temperature range from -30.0 to 0.0 ^{o}C by CO_2 evaporation process. In some important industrial applications, i.e. fishing industry and biomedical engineering, there is a strong demand for the refrigeration temperature below -30.0 ^{o}C.

To this aim, several years ago, an ultra-low temperature refrigeration system using CO_2 as a working fluid was introduced by our research group (Yamaguchi et al. 2008, 2009) and it has been shown to be able to achieve the temperature below the CO_2 triple-point temperature of -56^{o}C. The system is a cascade system comprised of two CO_2 refrigeration compression cycles, where one is a trans-critical cycle and another is a trans-triple-point

cycle. The temperature below the triple-point is realized by an expansion process of the liquid CO_2 into the dry ice and gas mixtures in an horizontal evaporator, an expansion tube, in the a trans-triple-point cycle (Fig. 1). The reason designing a cascade system is due to a low condensing temperature necessary for dry ice condensation in expanding process. This refrigeration system has been proved to be functional by experiments and theoretical analysis (Yamaguchi and Zhang, 2009) and has been shown to have capability of providing the users a cryogenic environment below -56.6 ^{o}C and thermal energy supply above 80 ^{o}C at the same time. In addition, parametric study based on visualizing the CO_2 dry ice behaviors in the evaporator of the system has also been carried out in order to get a longer duration of the deposition and a shorter duration of melting (Niu et al. 2010; Yamaguchi et al. 2011).

As the system refrigeration performance greatly depends on the thermodynamic properties of the CO_2 dry ice-gas mixture in the evaporator in the system, it is quite necessary to know the heat transfer behaviors of the CO_2 dry ice-gas flow in the evaporator so that the optimal operation condition of the system can be obtained. However, such kinds of studies have been scarcely studied in the past years and detailed information of the CO_2 dry ice-gas heat transfer and flow in the expansion tube is much lack (Zhang and Yamaguchi, 2011). As a continues series research works of our CO_2 ultra-low temperature refrigeration system, in the present study, an intensive experimental studies of the heat transfer behaviors of the CO_2 dry ice-gas flow in the evaporator of the system were carried out by varying condensation temperatures, rotational frequency of the compressor and opening of the expansion valve in the low-temperature cycle of the system. The rest of the

paper is organized as follows. In Sec. 2, details of the experiment are introduced. Sec. 3 is devoted to results and discussions of the present study. A conclusion is given in Sec. 4.

1. Experiment details

2.1 Experimental set-up

The CO_2 cascade refrigeration system is composed of two cycles (Yamaguchi and Zhang, 2009, Niu et al., 2011, Yamaguchi et al., 2011): a low temperature cycle (LTC) and a high temperature cycle (HTC). In the HTC, CO_2 is cooled to -20^{o}C through a reciprocating-type compressor (TCS350/4, Product of Officine Mario Dorin), two condensers (Tubular-type heat exchangers, Nippon Manufacture Co. Ltd.), a needle expansion valve (Product of Swagelok) and a plate-type evaporator (Product of Tokyo blaze Co., Ltd.). In the LTC, one more condenser is used and cooled by the brine from the evaporator of the HTC. Through three condensers in the LTC, CO_2 is cooled to below -20^{o}C and then expanded into the horizontal evaporator to achieve the dry ice-gas two-phase flow and obtain an ultra-low refrigeration temperature below the triple point (Fig. 1).

As the system refrigeration mainly depends on the performance of the LTC of the whole system, we are here only displaying the set-up of the LTC. Fig. 2 shows the sketch of the LTC of the system with pressure and temperature measuring points indicated. Particularly, we defined the temperature before the expansion valve as the condensation temperature $T_{\text{condensation}}$ in the present study. The details of the test section of the evaporator in the LTC are sketched in Fig. 2. The test section is a horizontal circular copper tube, which has an internal diameter of 0.04m and thickness of 0.0025m. The length of the test

section is 5.0 m. The inlet and outlet pipes have a same thickness of 0.0015m, and their diameters are 0.01588m and 0.02222m, respectively. The heater used to heat the tube is a silicon-gum-type heater with good water proof. The heater can be used in a low-temperature environment until -80^{o}C. In order to investigate the heat transport characteristics of CO_2 dry ice-gas two phase flow in the test section, four pressure measuring points (denoted as P_1-P_4) were arranged with uniformly distributed along the evaporator, and 13 outer wall temperature measuring points (denoted as T_1~T_{13}) were positioned along the evaporator by: three points at the entrance neighborhood with interval 200mm, ten points in the middle of test section with interval 400mm. In addition, temperatures at the inlet and outlet tubes were also measured and they were denoted as T_{in} and T_{out}, respectively.

2.2 Experimental implementation and measurements

To well understand the system performance during investigation, all measurements were taken after the whole system runs stably. In experiment, the HTC was started first to cool the brine (concentration 55%, melting point -30 ^{o}C) of second subsystem. After the brine was fully cooled, the heater (Maximum heat flux 4,244 W/m^2) rounded in the evaporator in the LTC was started to preheat the tube. When the evaporator in the LTC reached the prescribed temperature, the LTC was started. Then the two machine systems should be made to operate simultaneously. The stable state of the system operation was judged by observing whether temperatures and pressures before and after the compressor in the LTC converged into a confined range. In the present work, pressure and temperature

became steady around 3 hrs later from the HTC starting working.

In investigation, the flow rates of the cool and hot water at two condensers and the brine in the evaporator were kept at 7.0 l/min, 120 l/min and 50 l/min, respectively. To obtain optimized operation condition of the system and understand the heat transfer behaviors of CO_2 in the evaporator in the LTC, studies were carried out by mainly varying working conditions of the condensation temperature $T_{condensation}$, the expansion valve opening D_{valve} and the compressor rotational frequency $f_{compressor}$ in the LTC. The condensation temperature can be adjusted and controlled by the brine flow rate and temperature and so on in the HTC through the brine heat exchanger. The detailed test conditions are listed as follows:

- Case 1: $T_{condensation}$ = -20 ^{o}C, -25 ^{o}C and -30 ^{o}C; Heat flux of the heater: q = 1500 W (2652.5 W/m2); D_{valve} = 25 mm; $f_{compressor}$ = 60 Hz; Temperature of the cool water: T_{cw} = 15 ^{o}C.
- Case 2: $f_{compressor}$ = 45 Hz, 50 Hz, 55 Hz, 60 Hz, 65 Hz and 70 Hz;

  2.1: D_{valve} = 20 mm, q = 1909.9 W/m^2, T_{cw} = 15 ^{o}C and $T_{condensation}$ = -20 ^{o}C.

  2.2: D_{valve} = 15 mm, q = 1909.9 W/m^2, T_{cw} = 15 ^{o}C and $T_{condensation}$ = -20 ^{o}C
- Case 3: D_{valve} = 15 mm, 20 mm and 25 mm;

  3.1: $f_{compressor}$ = 50 Hz, q = 1909.9 W/m^2, T_{cw} = 15 ^{o}C and $T_{condensation}$ = -20 ^{o}C

  3.2: $f_{compressor}$ = 60 Hz, q = 1909.9 W/m^2, T_{cw} = 15 ^{o}C and $T_{condensation}$ = -20 ^{o}C

In measurement, T-type thermocouples with an uncertainty of 0.1^{o}C and pressure transmitter with an uncertainty of 0.2% were used for measuring temperature and pressure, respectively. All measured data were transferred into computer through distributor and data

logger. The sample data were obtained in every 5s.

2.3 Evaluations

In the present study, all analyses presented in this paper were based on the measured data of the wall temperatures and the CO_2 pressures along the test section tube. The pressure-bear material of the experimental set-up makes it difficult to measure the internal temperature of the tube. Here, the inside tube wall temperature is estimated based on a simple calculation, which is carried out on thermal resistance from the outside tube wall to the inside tube wall. Then this inside tube wall is used in estimating heat transfer characteristics. In addition, the liquid CO_2 becomes the dry ice-gas two-phase fluid after passing through the expansion valve and its pressure is reduced. As shown in the curve in Fig. 1, it is noted that the isotherm line is parallel to the horizontal axis in the dry ice-gas two-phase region, thus the saturation temperature values (T_{1in}, T_{2in}, T_{3in}, T_{4in}, Fig. 3 (b)) corresponding to the measured pressures (P_1-P_4) can be regarded as the internal CO_2 fluid temperature inside the test section tube. The CO_2 temperature between two pressure measurement points is obtained by averaging temperatures of the two points, which can also be seen in Fig. 3 (b). In this figure, a coordinate system x is also given, in which the origin point is located at the beginning of the test section. According to Newton's cooling law, the local heat transfer coefficient h is thus given by:

$$h = \frac{q}{T_w - T_{in}}, \tag{1}$$

where q [W/m^2] is the heat flux of the heater to the expansion tube, and T_w and T_{in} are the inner-wall temperature of the expansion tube and the CO_2 temperature in the tube, respectively.

3. Results & Discussions

Fig. 4 shows the distributions of the wall temperature T_w and the local heat transfer coefficient h along the evaporator in the LTC of the system at the condition of case 1. As shown of the wall temperature distribution in Fig. 4(left), for all three test condensation temperatures, T_w shows large variations in amplitude along the evaporator. This is mainly due to the fact that the dry ice particles are condensed and then sublimated and interactive with CO_2 gas flow in the evaporator tube. Particularly, it is seen that T_w rises slowly from x = 0 to x = 3500 [mm] along the evaporator, and increases rapidly after x = 35000 [mm]. It may be explained the CO_2 fluid sublimates in the region of x = 0~3500 [mm]. Because the sublimation process of dry ice absorbs a large amount of heat, the wall temperature rise cannot be obvious. After x = 3500 [mm], the CO_2 fluid may mainly be gas state, so the CO_2 temperature increases obviously when the tube is heated. In this region, the non-equilibrium effects may dominate and the CO_2 vapor temperature increases and exceeds the sublimation temperature in the dry ice particles. Moreover, our early studies (Niu et al. 2010; Yamaguchi et al. 2011; Zhang & Yamaguchi, 2011) showed that, with $T_{condensation}$ reducing, the refrigeration temperature in the evaporator tube in the LTC of the system decreases. This can also be evidenced by the local wall temperature distribution in Fig. 4 (left), which demonstrates T_w decreasing with $T_{condensation}$ reducing, and the sublimation length becomes

longer when $T_{condensation}$ is lower, implying that the CO_2 particle sublimation become slower if $T_{condensation}$ is decreased.

Based on the wall temperature distributions, the local heat transfer coefficients h at the condition of Case 1 is shown in Fig. 4 (right). In the present measurement, the accuracy of the local heat transfer coefficients h and other all the parameters are calculated to be less than ±3.0% using the uncertainty analysis (Yamaguchi and Zhang, 2009). From this figure, it is seen that the local heat transfer coefficients h also vary in amplitude along the evaporator tube and is relatively flat with slightly decrease in the region of x = 0~3500 [mm]. It may be physically explained that, in this region the dry ice condensation and sublimation behavior makes the CO_2 flow field complicated: i. e., the dry ice particle accumulation impedes the flow and the dry ice sublimation makes the thermal boundary layer thinner. The above reasons may contribute to the phenomena of the heat transfer variation and slightly decrease in the region of x = 0~3500 [mm]. After x = 3500 [mm], the local heat transfer coefficient has a larger oscillation and general trend is decreasing, which should be attributed to the flow in gas state and the development of the thermal boundary layer of the flow. Moreover, the local heat transfer coefficients h becomes larger when $T_{condensation}$ reducing, which slows the dry ice sublimation rate.

Figs. 5 and 6 show the distributions of T_w and h of $f_{compressor}$ = 50, 60 and 70 [Hz] along the evaporator in the LTC of the system at the conditions of cases 2.1 and 2.2, respectively. It is observed from Figs. 5 and 6 that the distributions of T_w and h of $f_{compressor}$ = 50, 60 and 70 [Hz] along the evaporator show similar behaviors to those in Fig. 4. However, compared to Fig. 4, T_w and h in these two figures show smaller amplitude variations along the

evaporator due to D_{valve} and q in these tests reducing, which implies the dry ice sublimation rate decreases. As shown in Fig. 5, the effect of $f_{compressor}$ to the heat transfer of the CO_2 dry ice-gas two-phase flow in the evaporator is complicated: when $f_{compressor}$ increases from 50 to 60 [Hz], T_w decreases and thus h increases; but when $f_{compressor}$ increases further from 60 to 70 [Hz], T_w increases again and thus h decreases again. These phenomena can be explained by two reasons; one is that the dry ice sublimation in the evaporator increases from $f_{compressor}$ = 50 to 60 [Hz] and decreases from $f_{compressor}$ = 60 to 70 [Hz]; the other is that the dry ice particles may be more clustered in the evaporator tube and block the flow passage at $f_{compressor}$ = 60 to 70 [Hz] than they are at $f_{compressor}$ = 50 to 60 [Hz]. The effect of dry ice cluster reducing flow passage can be more demonstrated in Fig. 6, by reducing D_{valve} further to 15 mm, the dry ice should be more clustered resulting T_w increasing when $f_{compressor}$ increases from 50 to 70 [Hz] and further leading to h decreases.

The effects of D_{valve} on the local heat transfer of the CO_2 dry ice-gas two-phase flow in the evaporator are further examined in Figs. 7 and 8, which show T_w and h of D_{valve} = 15, 20 and 25 [mm] along the evaporator in the LTC of the system at the conditions of Cases 3.1 and 3.2, respectively. From Figs. 7 and 8, one can observed opposite heat transfer behaviors at $f_{compressor}$ = 50 and 60 [Hz] by varying D_{valve}. At $f_{compressor}$ = 50 Hz, T_w decreases and h increases with reducing D_{valve}. However, at $f_{compressor}$ = 60 Hz, T_w increases and h decreases with reducing D_{valve}. These phenomena illustrate that, although increasing $f_{compressor}$ increases the CO_2 flow rate in the LTC and hence should improve the refrigeration and heat transfer of the CO_2 dry ice-gas two-phase flow in the evaporator, reducing D_{valve} makes the dry ice sublimation slower and more dry ice particles are clustered to inhibit the

heat transfer of the flow in the evaporator; when the effect of the dry ice particles is over that of the increased $f_{compressor}$, the local heat transfer of the CO_2 dry ice-gas two-phase flow decreases.

4. Conclusions

In this study, a series experimental studies of the heat transfer characteristics of the CO_2 dry ice-gas flow in the evaporator of a CO_2 ultra-low temperature cascade refrigeration system was performed by varying condensation temperatures, rotational frequency of the compressor and opening of the expansion valve in the low temperature cycle of the system.

From the present study, we found that the local heat transfer coefficient and wall temperature along the evaporator show greatly complicated behaviors due to the fact that the dry ice particles are condensed, sublimated and interactive with CO_2 gas flow in the evaporator tube. In the experimented range of this study, the CO_2 sublimation process is measured to occur within x = 0 to 3500 [mm], in which the wall temperature is observed to vary in amplitude and keeps slightly increase trend under the test conditions. After x = 3500[mm], the wall temperature seems to increase obviously along the evaporator tube. At the same time, the local heat transfer coefficients are observed to also vary in amplitude but keeps slightly decrease trend in the region of x = 0 to 3500 [mm] under the test conditions. After x = 3500 [mm], the local heat transfer coefficient has a larger oscillation and general trend is decreasing, which should be attributed to the flow in gas state and the development of the thermal boundary layer of the flow. Moreover, the local heat transfer coefficients can be enhanced by reducing the condensation temperature. However, the effect of the rotational frequency of the compressor and the openings of the expansion valve on the local

heat transfer are very complicated due to the dry ice sublimation and cluster in the evaporator tube.

References

ASHRAE Handbook-Fundamentals (I-P edition, American Society of Heating, Refrigerating and Air-Conditioning Engineers, Inc., 2009)

Cecchinato, L., Corradi, M., Fornasieri, E., Zamboni, L., 2005. Carbon dioxide as refrigerant for tap water heat pumps: a comparison with the traditional solution. International Journal of Refrigeration 28, 1250–1258.

Girotto, S., Minetto, S., Neksa, P., 2004. Commercial refrigeration system using CO_2 as the refrigerant. International Journal of Refrigeration 27, 717–723.

Hafner, A., Pettersen, J., Skaugen, G., Nekså, P., 1998. An automobile HVAC system with CO_2 as the refrigerant. In: IIR-Third IIR-Gustav Lorentzen Conference on Natural Working Fluids, June 2–5, 1998, Oslo, Norway.

Kim, M.H., Pettersen, J., Bullard, C.W., 2004. Fundamental process and system design issues in CO_2 vapor compression systems. Progress in Energy and Combustion Science 30, 119–174.

Kim, S.C., Won, J.P., Park, Y.S., Lim, T.W., Kim, M.S., 2009. Performance evaluation of a stack cooling system using CO_2 air conditioner in fuel cell vehicles. International Journal of Refrigeration 32, 70–77.

Liao, S. M., and Zhao, T. S., 2002. An experimental investigation of convection heat transfer to supercritical carbon dioxide in miniature tubes. Int. J. Heat Mass Transfer, 45, 5025-5034.

Lorentzen, G., 1990. Trans-critical Vapour Compression Cycle Device, International Patent Publication WO 90/07683.

Lorentzen, G., 1993. Large heat pumps using CO_2 as refrigerant. In: IIR Energy Efficiency in Refrigeration and Global Warming Impact, May 12–14, 1993, Gent, Belgium.

Lorentzen, G., 1994. Revival of carbon dioxide as a refrigerant. International Journal of Refrigeration 17, 292–301.

Nekså, P., Girotto, S., Schiefloe, P.A., 1998. Commercial refrigeration using CO_2 as refrigerant-system design and experimental results. In: IIR-Third IIR-Gustav Lorentzen Conference on Natural Working Fluids, June 2–5, 1998, Oslo, Norway.

Nekså, P., 2002. CO_2 heat pump systems. International Journal of Refrigeration 25, 421–427.

Niu, X.-D., Yamaguchi, H., Sekimoto, K., Nekså, P., 2010. Experimental study on a CO_2-solid-gas-flow-based ultra-low temperature cascade refrigeration system, International Journal of Low Carbon Technology 0, 1-7.

Rieberer, R., 2005. Naturally circulating probes and collectors for ground-coupled heat pumps. International Journal of Refrigeration 28, 1308–1315.

Saikawa, M., 2004. Development of Home CO_2 Heat Pump Hot Water Supplying Apparatus, Science of Machine 56, 446-451.

Stene, J., 2005. Residential CO_2 heat pump system for combined space heating and hot

water heating. International Journal of Refrigeration 28, 1259–1265.

Yamaguchi, H., Niu, X.-D., Sekimoto, K., Nekså, P., 2011. Investigation of dry ice blockage in an ultra-low temperature cascade refrigeration system using CO_2 as a working fluid. International Journal of refrigeration 34, 466-475.

Yamaguchi, H., Zhang, X.R., Fujima, K., 2008. Basic study on new cryogenic refrigeration using CO_2 solid–gas two phase flow. International Journal of Refrigeration 31, 404–410.

Yamaguchi, H., Zhang, X.R., 2009. A novel CO_2 refrigeration system achieved by CO_2 solid–gas two-phase fluid and its basic study on system performance. International Journal of Refrigeration 32, 1683–1693.

Zhang, X.R., Yamaguchi, H., 2011, An experimental study on heat transfer of CO2 solid-gas two phase flow with dry ice sublimation. International Journal of Thermal Sciences 50, 2228-2234.

Zhang, X.R., Yamaguchi, H., 2007, Forced convection heat transfer of supercritical carbon dioxide in a horizontal circular tube. Journal of Supercritical Fluids 41, 412-420.

Zhang, X.R., Yamaguchi, H., Fujima, K., Enomoto, M., Sawada, N., 2005. A feasibility study of CO_2-based Rankine cycle powered by solar energy. JSME International Journal – Series B: Fluids and Thermal Engineering 48, 540–547.

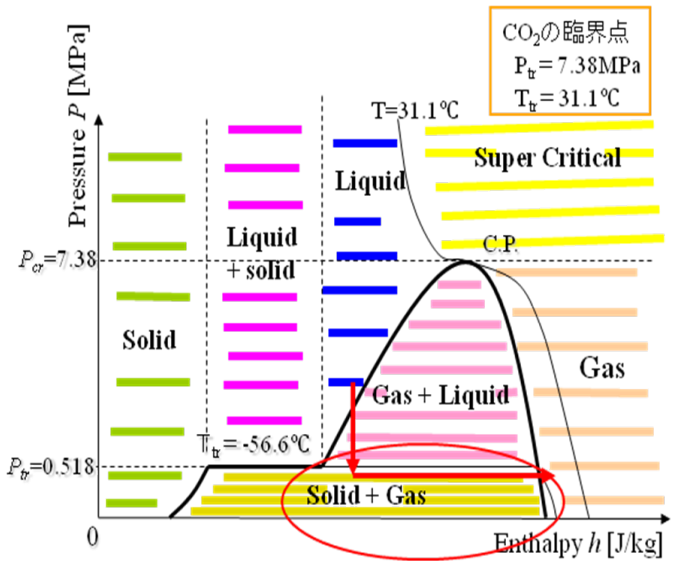

Fig. 1 Principle schematic of the refrigeration method using CO_2 dry ice-gas two phase fluid flow: CO_2 *P-h* diagram.

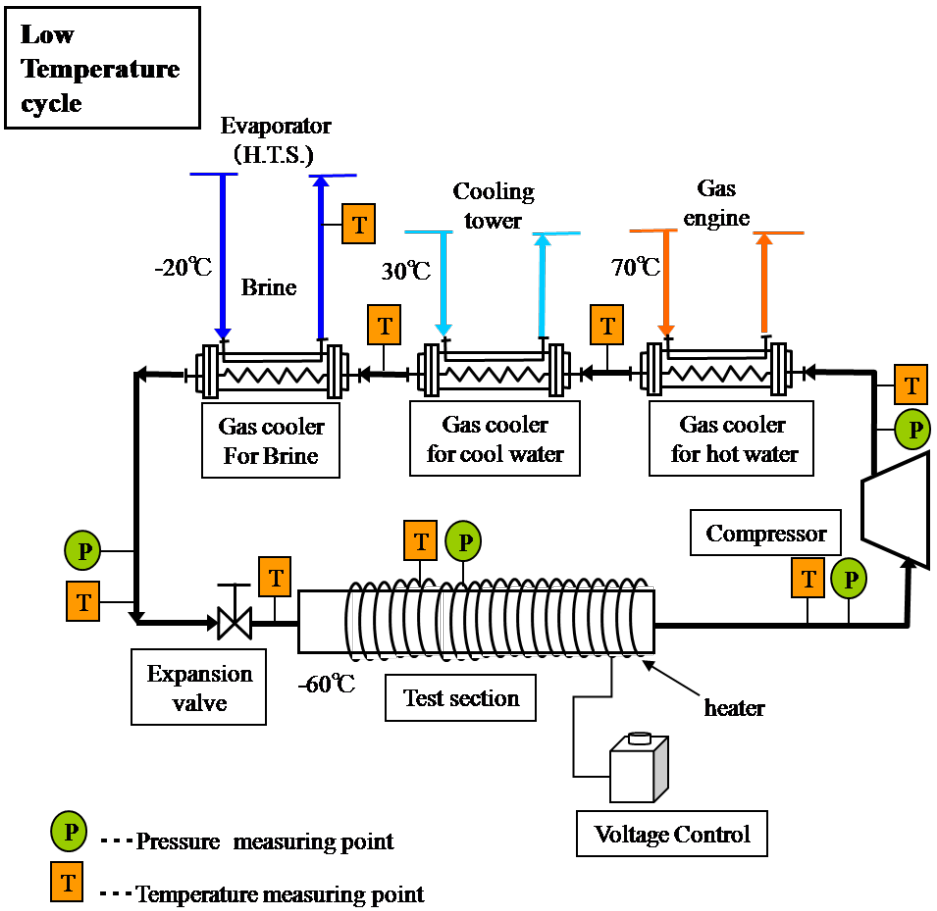

Fig. 2 Schematic of the low temperature cycle (LTC) of the CO_2 cascade refrigeration system

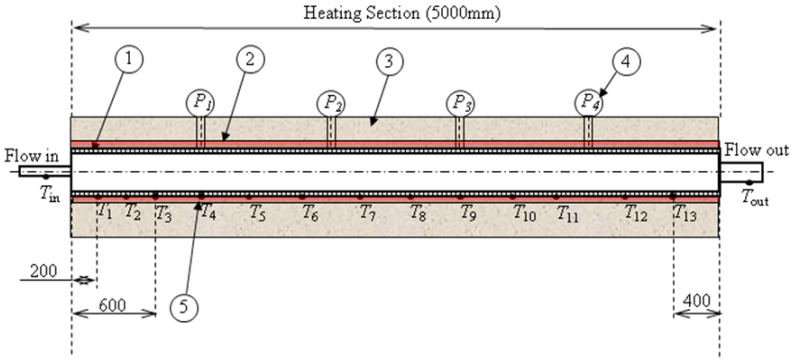

① Copper pipe (d=40mm, t=2.5mm, L=5000mm)
② Heater (silicon rubber)
③ Glass-wool insulation (150mm)
④ Pressure transducer (4 points, uniformly distributing along test section)
⑤ Thermocouple (15 points)

(a) Details of test section

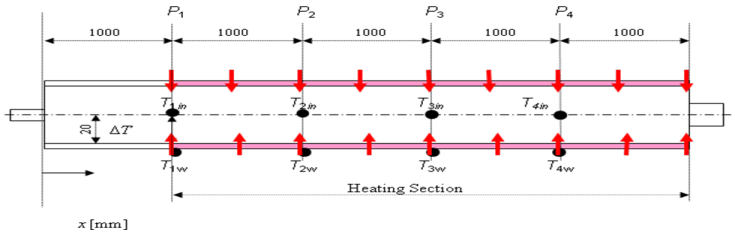

(b) Wall and inside temperatures

Fig. 3 Schematic of the test section and pressure and temperature measurement positions along the test section.

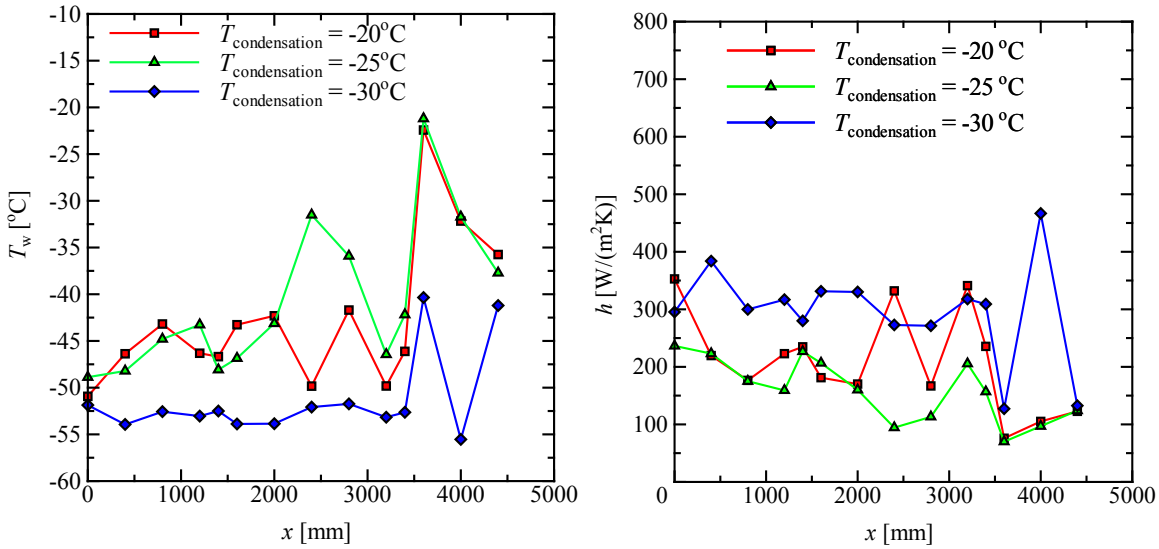

Fig. 4 Wall temperature (left) and local heat transfer coefficient (right) and of three condensation temperatures along the expansion tube (q = 2652.5 W/m^2; D_{valve} = 25 mm; T_{cw} = 15 °C; $f_{compressor}$ = 60 Hz).

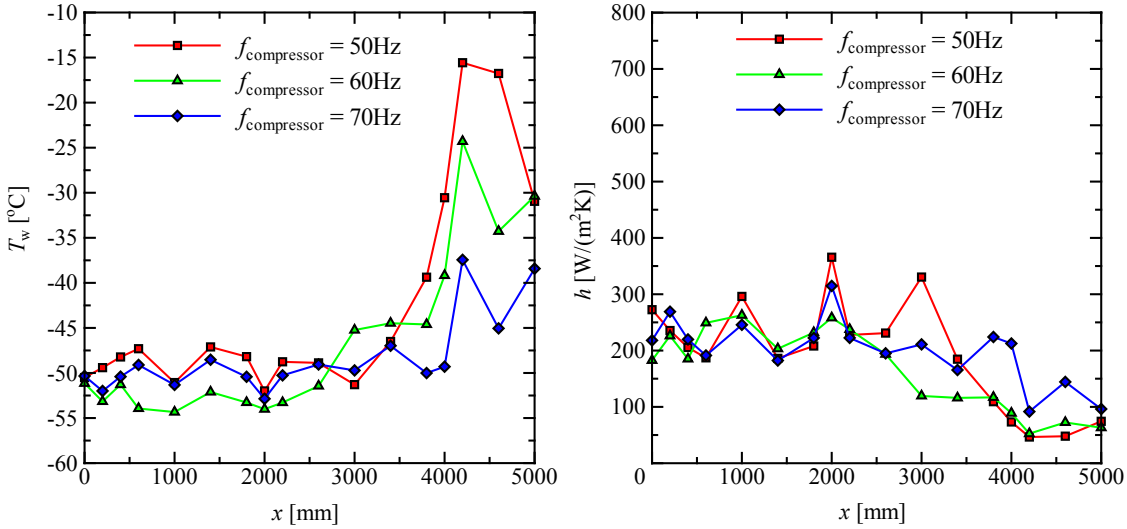

Fig. 5 The wall temperature (left) and heat transfer coefficient (right) of three rotational frequencies of the compressor along the expansion tube (q = 1909.9 W/m^2; D_{valve} = 20 mm; T_{cw} = 15 °C; $T_{condensation}$ = -20 °C)

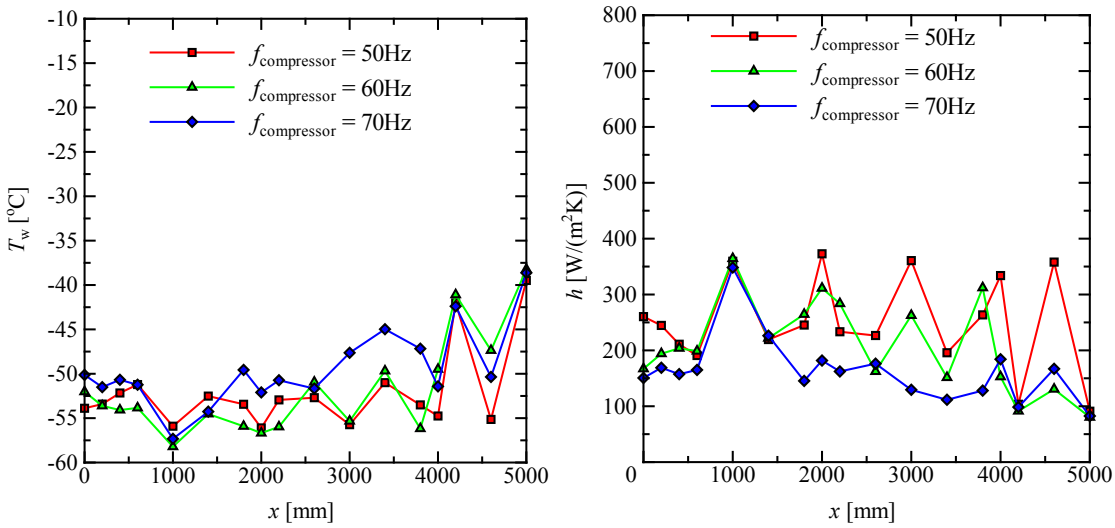

Fig. 6 The wall temperature (left) and heat transfer coefficient (right) of three rotational frequencies of the compressor along the expansion tube (q = 1909.9 W/m^2; D_{valve} = 15 mm; T_{cw} = 15 °C; $T_{condensation}$ = -20 °C)

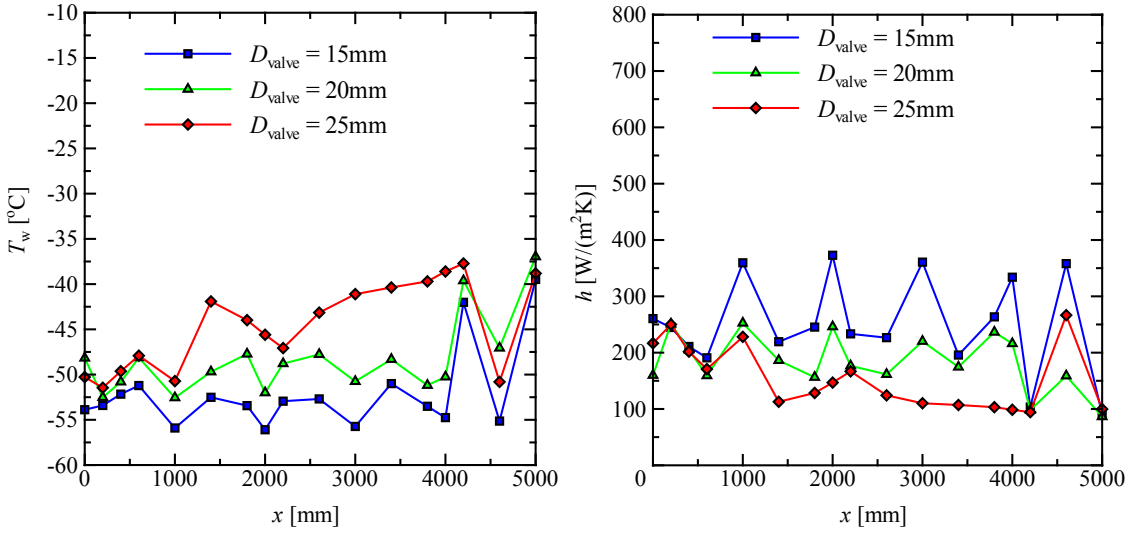

Fig. 7 The wall temperature (left) and heat transfer coefficient (right) of three expansion valve openings along the expansion tube (q = 1909.9 W/m^2; $f_{compressor}$ = 50 Hz; T_{cw} = 15 °C; $T_{condensation}$ = −20 °C).

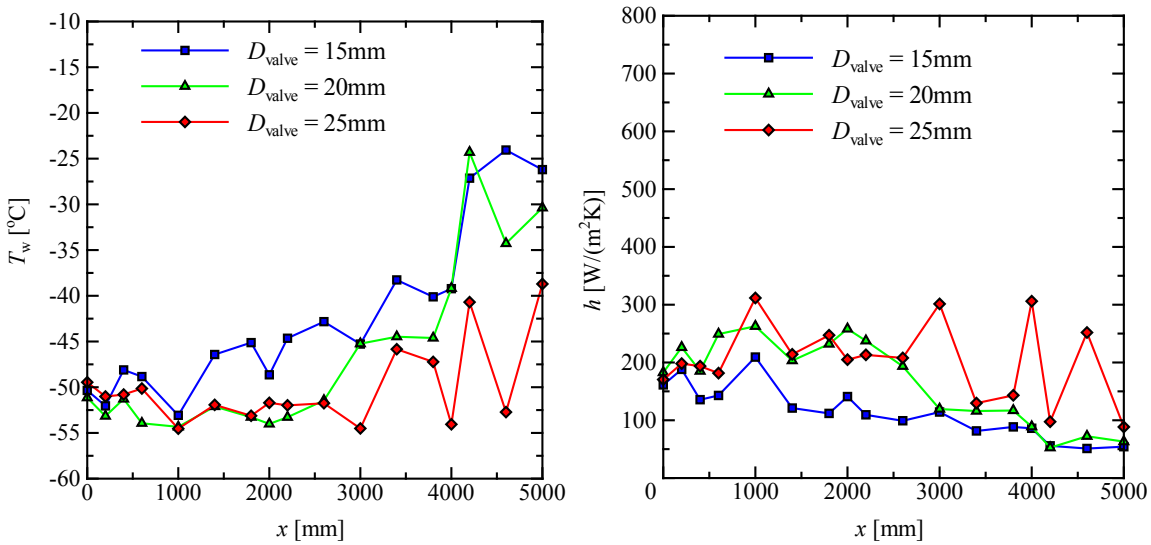

Fig. 8 The wall temperature (left) and heat transfer coefficient (right) of three expansion valve openings along the expansion tube (q = 1909.9 W/m^2; $f_{compressor}$ = 60 Hz; T_{cw} = 15 °C; $T_{condensation}$ = −20 °C).